Optical and Quantum Electronics (2023) 55:995
https://doi.org/10.1007/s11082-023-05235-4

All optical switching in a three-level V-type atomic medium based on electromagnetically induced transparency

Hoang Minh Dong[1] · Nguyen Huy Bang[2] · Le Van Doai[2] · Luong Thi Yen Nga[2]

Received: 24 April 2023 / Accepted: 27 July 2023

Abstract
We use electromagnetically induced transparency (EIT) to generate optical switching of the probe laser field according to the pulse modulation of the coupling laser field in a three-level V-type atomic system. When the absence of the coupling laser field, the probe laser field is completely absorbed by the atomic medium at the resonant frequency. However, the probe laser field becomes transparent when the coupling laser field is present. Thus, by turning the coupling laser field ON or OFF, the output signal of the probe laser field is also switched from ON to OFF, and vice versa. To describe this optical switching phenomenon, we derive a set of Maxwell–Bloch equations for the three-level V-type atomic system with laser fields and use a combination of the four-order Runge–Kutta and finite difference numerical methods to simulate the propagation of the probe and coupling laser pulses in the atomic medium. Under the EIT condition, we obtain the optical switching of the probe pulse that modulated according to the coupling pulse. The influence of the switching period as well as the intensity and frequency of the coupling laser field on the optical switching of the probe laser field are also studied.

Keywords Electromagnetically induced transparency · All optical switching · Pulse propagation

✉ Luong Thi Yen Nga
ngalty@vinhuni.edu.vn

Hoang Minh Dong
dong.gtvtmt@gmail.com

Nguyen Huy Bang
bangnh@vinuuni.edu.vn

Le Van Doai
doailv@vinhuni.edu.vn

[1] Ho Chi Minh City University of Industry and Trade, Ho Chi Minh City, Vietnam

[2] Vinh Universiy, Vinh City, Vietnam

Published online: 13 September 2023

1 Introduction

All-optical switching is an important element in optical network communications and optical storage devices (Ishikawa 2008). In recent years, researchers have always desired to find materials that can create optical switching with tunable switching characteristics and high switching speed. However, it is often difficult to achieve in traditional nonlinear materials due to saturation effects. Currently, an excellent solution to suppress saturation effects is to use the EIT effect (Boller et al. 1991). The EIT materials not only possess zero absorption but also have giant nonlinearity (Wang et al. 2001; Khoa et al. 2014; Bai and Huang 2016). Therefore, a lot of nonlinear optical effects can be observed with very low light intensities, even with a single photon (Ying et al. 2014; Khoa et al. 2017a; Bang et al. 2019).

With such extraordinary properties of EIT materials, it has been used to help laser pulses propagate in the atomic medium without attenuation or distortion (i.e., soliton pulses are easily generated) (Eberly 1995; Harris and Luo 1995; Huang et al. 2006; Si et al. 2010). The first studies of undistorted pulse propagation in the EIT medium of the three-level lambda atomic system were proposed by Eberly (Eberly 1995) and Harris (Harris and Luo 1995). Since then, studies of propagation of soliton-like pulses (Buica and Nakajima 2014), adiabatic propagation of short pulses (Dong et al. 2016a), dynamical control of light pulse propagation (Kasapi et al. 1995; Wan et al. 2010; Kiffner and Dey 2009), propagation of ultraslow optical solitons (Arkhipkin and Timofeev 2000), tunable single-photon pulses (Eisaman et al. 2005), laser pulse propagation in inhomogeneously broadened three-level cascade atomic medium (Khoa et al. 2017b; Dong et al. 2016b), pulse propagation in an atomic medium under spontaneously generated coherence, incoherent pumping, and relative laser phase (Dong et al. 2018) have also been published recently.

Laser pulse propagation as optical solitons in the presence of EIT or it is completely absorbed by the medium in the absence of EIT, is the basis for creating all-optical switching with controllable threshold intensity and switching speed. Indeed, Schmidt et al. (Schmidt and Ram 2000) presented an all-optical switching based on absorption modulation in a three-level system. Brown et al. (Brown and Xiao 2005) demonstrated an all-optical two-port signal router-all-optical switch based on an electromagnetically induced absorption grating. Yavuz et al. (Yavuz 2006) proposed a full optical conversion technique using two-photon absorption of a three-level atomic system. Wei et al. (2010) experimentally observed all-optical switching in a cavity QED system consisting of three-level Λ-type atoms and show that the transmission of a signal light through the cavity is switched on or off by a control laser. Antón et al. (2008) obtained all-optical switching in a five-level N-tripod-type atom. Yu et al. (2009) studied the control of propagation dynamics and the optical switching of a four-level atomic medium by an external radio field. Paspalakis et al. (2010) investigated the implementation of all-optical modulation in three-level Λ-type quantum systems and demonstrated its dependence on the applied laser field and atomic parameters. Qi et al. (2011) showed that the switching action of the probe laser pulse can be realized by adjusting the phase or intensity of the coupling fields in a four-level atomic system (Qi et al. 2013). Li et al. (2013) presented pulse propagation and optical switching in a four-level inverted Y atom medium. Most recently, Dong et al. (2019), Dong and Bang (2019), Anh et al. (2021), Doai et al. (2018) have presented optical switching based on external magnetic fields. However, these proposed models often use two laser fields for EIT generation and optical switching of the probe laser field independently. As we known that, the basic configurations of EIT are three-level atomic systems consisting of lambda, ladder and V-type diagrams which excited by a probe laser field and a coupling laser field (Harris 1997; Wu and Yang 2005). The presence of the coupling field can lead to the transition

between absorption and transparency regimes of the atomic medium, and thus the coupling field can be used to generate EIT as well as optical switching for the probe field.

In this work, we study EIT-based all-optical switching under pulse regime in a three-level V-type scheme by numerically solving Maxwell-Bloch equations on a space–time grid. It is easily switch between transparency and absorption regimes of the medium by turning on or off the coupling laser so that it is easy to create optical switching for the probe field. The advantage of this model is that it only uses the single coupling laser field to generate both the EIT and optical switching for the probe laser field. In addition, the influence of the laser parameters as well as the switching period on the switching efficiency is also considered.

2 Theoretical model and basic equations

Let us consider a three-level V-type atomic system excited by two laser fields, as shown in Fig. 1. The transition $|1\rangle \leftrightarrow |3\rangle$ is driven by a strong coupling field (with carrier frequency ω_c and Rabi frequency Ω_c), while the transition $|1\rangle \leftrightarrow |2\rangle$ is driven by a weak probe field (with carrier frequency ω_p with Rabi frequency Ω_p). The decay rates of the states $|2\rangle$ and $|3\rangle$ are denoted γ_{21} and γ_{31}, respectively.

Using the semiclassical theory with the dipole and rotating wave approximations, the density matrix equations of motion for the three-level V-type system in laser fields can be written as:

$$\dot{\rho}_{11} = \gamma_{21}\rho_{22} + \gamma_{31}\rho_{33} + \frac{i}{2}\Omega_c(\rho_{31} - \rho_{13}) + \frac{i}{2}\Omega_p(\rho_{21} - \rho_{12}) \tag{1}$$

$$\dot{\rho}_{22} = -\gamma_{21}\rho_{22} + \frac{i}{2}\Omega_p(\rho_{12} - \rho_{21}) \tag{2}$$

$$\dot{\rho}_{33} = -\gamma_{31}\rho_{33} + \frac{i}{2}\Omega_c(\rho_{13} - \rho_{31}) \tag{3}$$

$$\dot{\rho}_{21} = -\left(i\Delta_p + \frac{\gamma_{21}}{2}\right)\rho_{21} + \frac{i}{2}\Omega_p(\rho_{11} - \rho_{22}) - \frac{i}{2}\Omega_c\rho_{23} \tag{4}$$

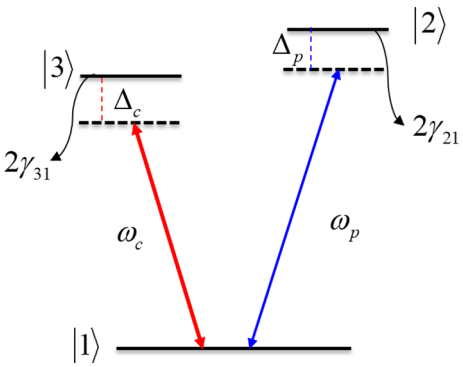

Fig. 1 Schematic model of a three-level V-type atom system interacting with laser fields

$$\dot{\rho}_{23} = -\left[i(\Delta_p - \Delta_c) + \frac{\gamma_{31} + \gamma_{21}}{2}\right]\rho_{23} - \frac{i}{2}\Omega_c\rho_{21} + \frac{i}{2}\Omega_p\rho_{13} \tag{5}$$

$$\dot{\rho}_{31} = -\left(i\Delta_c + \frac{\gamma_{31}}{2}\right)\rho_{31} + \frac{i}{2}\Omega_c\left(\rho_{11} - \rho_{33}\right) - \frac{i}{2}\Omega_p\rho_{32}. \tag{6}$$

$$\text{with } \rho_{ij} = \rho_{ji}^{*}(i \neq j), \text{and } \rho_{11} + \rho_{22} + \rho_{33} = 1 \tag{7}$$

where $\Delta_p = \omega_p - \omega_{21}$ and $\Delta_c = \omega_c - \omega_{31}$ are the frequency detuning of the probe and coupling laser fields, respectively.

3 Results and discussion

3.1 Probe absorption behaviors under EIT

The model of three-level V-type atomic system can be applied to the ^{87}Rb atom with the designated states chosen as: $|1\rangle = |5S_{1/2}, F = 1\rangle$, $|2\rangle = |5P_{3/2}, F' = 2\rangle$, $|3\rangle = |5P_{1/2}, F' = 2\rangle$. The atomic parameters are given by: $\gamma_{21} = 6$ MHz, $\gamma_{31} = \gamma_{21}$, $\lambda_p = 780$ nm, $\lambda_c = 795$ nm. For simplicity, all quantities related to the frequency are scaled by γ_{21}.

Firstly, we discuss the influence of the coupling field on the absorption and dispersion properties of the medium for the probe field by numerically solving the density matrix Eqs. (1)–(7) in the steady regime. At the result, we obtain the density matrix solution ρ_{21} which is related to the linear susceptibility of the medium by the following relation:

$$\chi = \frac{2Nd_{21}^2}{\varepsilon_0\hbar\Omega_p}\rho_{21} \tag{8}$$

where N is the density of atoms, d_{21} is the dipole moment between the states $|1\rangle$ and $|2\rangle$, ε_0 is the free space permittivity. The imaginary $\mathrm{Im}(\chi)$ and real $\mathrm{Re}(\chi)$ parts of the linear susceptibility represent the absorption and dispersion coefficients of the atomic medium for the probe field, respectively. In Fig. 2, we have plotted the absorption $\mathrm{Im}(\chi)$ and dispersion $\mathrm{Re}(\chi)$versus the frequency detuning of the probe laser at different values of the coupling laser intensity: $\Omega_c = 0$ (a), $\Omega_c = 2\gamma_{21}$ (b), $\Omega_c = 5\gamma_{21}$ (c) and $\Omega_c = 10\gamma_{21}$ (d).

From the solid line in Fig. 2, we see that when the coupling laser beam is turned off ($\Omega_c = 0$), the probe laser beam is completely absorbed by the medium in the resonance region (see Fig. 2a). However, when the coupling laser beam is turned on, a hole appears on the absorption profile of the probe laser beam (called the EIT window) (see Fig. 2b). By gradually increasing the intensity of laser coupling, the depth and width of the EIT window are also increased (see Fig. 2b, c). However, when the coupling laser intensity is large enough, the depth of the EIT window is achieved to the maximum, so the continuous increase of the coupling laser intensity only increases the EIT window width (see Fig. 2c, d). Thus, by turning the coupling laser beam on or off, the probe laser beam can be completely transmitted or completely absorbed by the atomic medium. This is the fundamental principle for creating optical switching in dynamic pulse propagation mode. On the other hand, when EIT is established, the dispersion is also changed from anomalous dispersion (Fig. 2a) to normal dispersion (Fig. 2b). At the same time, when the depth and width of the EIT window are large enough (as in Fig. 2d), the dispersion curve also becomes zero

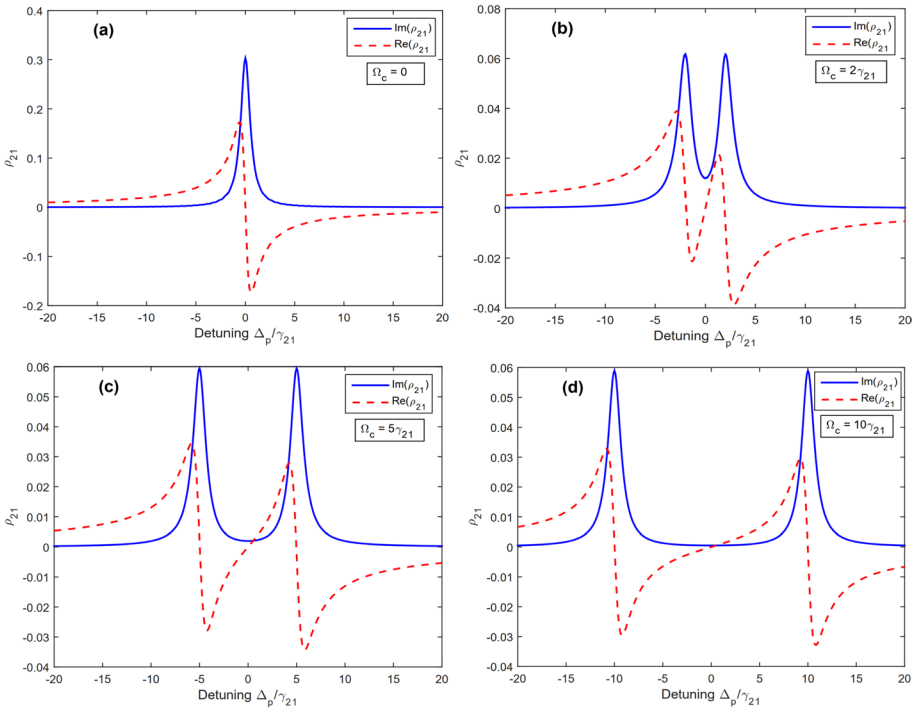

Fig. 2 Graphs of the absorption (solid line) and dispersion (dashed line) coefficients versus the probe detuning at different coupling laser intensities: **a** $\Omega_c = 0$, **b** $\Omega_c = 2\gamma_{21}$, **c** $\Omega_c = 5\gamma_{21}$, and **d** $\Omega_c = 10\gamma_{21}$. The other parameters are given by $\Omega_p = 0.2\gamma_{21}$ and $\Delta_c = 0$

dispersion at the center of the EIT window. This makes it possible for the light pulse propagation in the EIT window region to be undistorted (i.e., it retains a soliton pulse shape when leaving the medium) (Khoa et al. 2017b).

3.2 All optical switching

Next, we consider the propagation dynamics of probe laser field in the three-level V-type atomic medium under the EIT condition by deriving the one-dimensional wave propagation equation from the Maxwell wave equations in the slowly varying envelope approximation, as follows:

$$\frac{\partial \Omega_p(z,t)}{\partial z} + \frac{1}{c}\frac{\partial \Omega_p(z,t)}{\partial t} = i\alpha\rho_{21}(z,t) \tag{9}$$

where $\alpha = \frac{\omega_p N |d_{21}|^2}{4\epsilon_0 c\hbar}$ is the propagation constant. It is easier to transform the density matrix Eqs. (1)–(7) and the wave Eq. (9) in the local frame by setting $\xi = z$ and $\tau = t - z/c$, where c is the speed of light in the vacuum. In this frame, Eqs. (1)–(7) will be the same with the substitution $t \to \tau$ and $z \to \xi$, while Eq. (9) are rewritten as:

$$\frac{\partial \Omega_p(\xi,\tau)}{\partial \xi} = i\alpha\rho_{21}(\xi,\tau) \tag{10}$$

For convenience, we represent the probe Rabi frequency by $\Omega_p(\xi,\tau) = \Omega_{p0} f(\xi,\tau)$ where Ω_{p0} is a real constant indicating the maximum value of the probe Rabi frequency at the entrance of the medium ($\xi = 0$), and $f(\xi,\tau)$ is a dimensionless spatiotemporal pulse-shaped function. Therefore, Eq. (10) can be rewritten as:

$$\frac{\partial f(\xi,\tau)}{\partial(\alpha\xi)} = i\frac{\rho_{21}(\xi,\tau)}{\Omega_{p0}} \tag{11}$$

In order to simulate the propagation dynamics of probe laser field we numerically solve the coupled Bloch-Maxwell Eqs. (1)–(7), and (11) on a space–time grid by a combination of the four-order Runge–Kutta and finite difference mumerical methods with a computer code is developed from previous works (Dong et al. 2019; Dong and Bang 2019; Anh et al. 2021). For the initial condition at which all atoms are assumed in the ground state $|1\rangle$ [i.e., $\rho_{11}(\xi,\tau=0)=1$, $\rho_{22}(\xi,\tau=0)=0$, $\rho_{33}(\xi,\tau=0)=0$, and $\rho_{ij}(\xi,\tau=0)=0$ for $i\neq j$ (i, j = 1, 2,3)], and for the boundary condition at which the initial probe field having a Gaussian-type shape $f(\xi=0,\tau) = exp[-(ln2)(\tau-30)^2/\tau_0^2]$, with $\tau_o = 6/\gamma_{21}$ being the temporal width of the pulse at the entrance of the medium.

In Fig. 3, we have plotted spatiotemporal evolution of probe field intensity at different coupling field intensities $\Omega_c = 0$ (a) and $\Omega_c = 10\gamma_{21}$ (b) with $\Delta_c = \Delta_p = 0$. When the coupling field is turned off ($\Omega_c = 0$), the probe pulse is completely absorbed by the medium, even over a very short propagation distance (Fig. 3a). When the coupling field is turned on ($\Omega_c = 10\gamma_{21}$), the atomic medium is transparent to the probe pulse, and thus the probe pulse retains its shape over a long distance (Fig. 3b). This phenomenon is completely consistent with the absorption or transparency behavior of the probe beam in Fig. 2 above. This again demonstrates that by turning the coupling field on or off, the probe field can be completely transmitted or completely attenuated by the medium. Thus, if the coupling field is modulated to a square pulse with amplitude normalized by 0 and 1, then the probe field is also modulated accordingly. This will be demonstrated in Figs. 4, 5, 6 below.

In order to see the switching of the probe field in terms of the coupling field, we assume that probe field is a continuous wave (cw) and the coupling field is modulated by a near square pulse of the form:

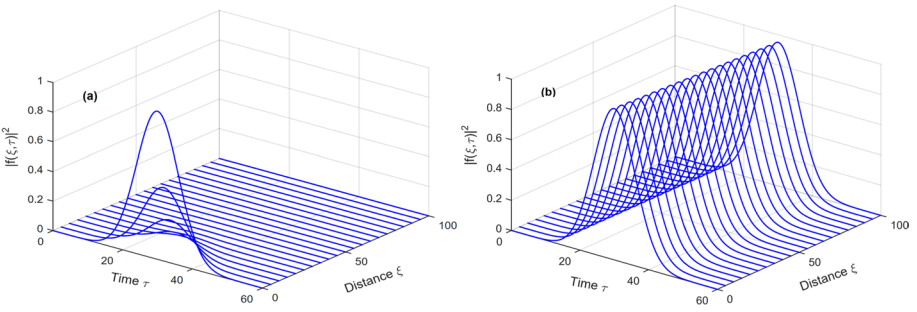

Fig. 3 Space–time evolution of the probe pulse intensity when the coupling field is turned off at $\Omega_c = 0$ (**a**) and turned on at $\Omega_c = 10\gamma_{21}$ (**b**). The other parameters are given by $\Omega_{p0} = 0.2\gamma_{21}$ and $\Delta_p = \Delta_c = 0$

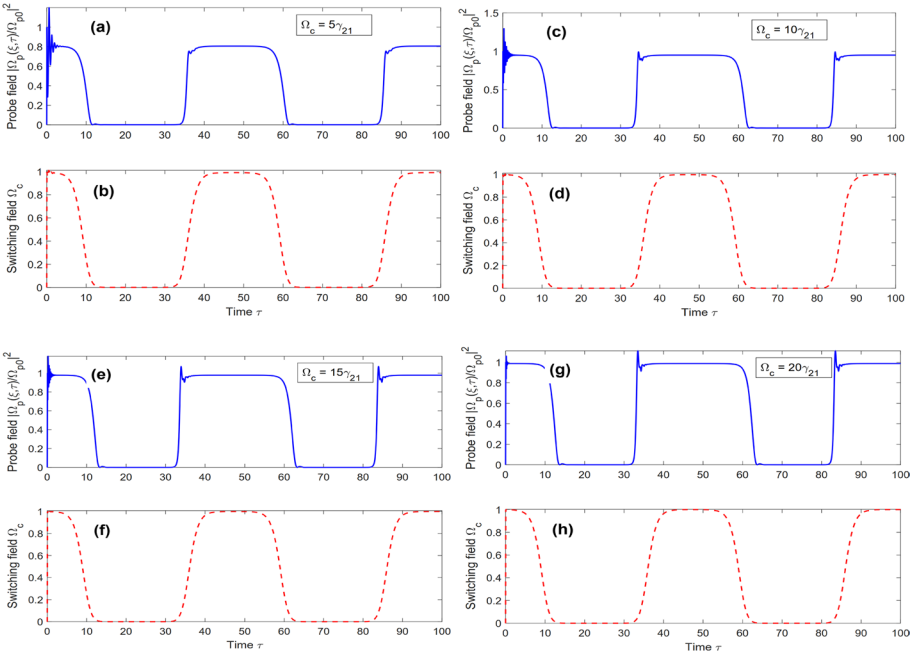

Fig. 4 Time evolution of the probe laser field (solid line) under the coupling laser modulation (dashed line) at different coupling laser intensities: $\Omega_{c0}=5\gamma_{21}$ (**a**, **b**), $\Omega_{c0}=10\gamma_{21}$ (**c**, **d**), $\Omega_{c0}=15\gamma_{21}$ (**e**, **f**), and $\Omega_{c0}=20\gamma_{21}$ (**g**, **h**). The other parameters are given by $\Omega_{p0}=0.2\gamma_{21}$, $\Delta_p=\Delta_c=0$ and period as $50/\gamma_{21}$

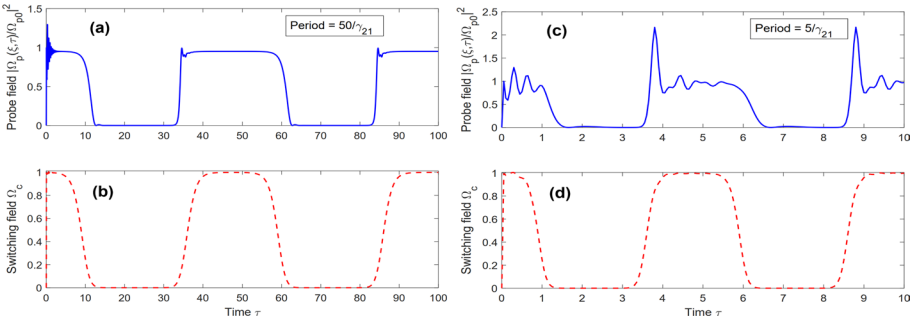

Fig. 5 Time evolution of the probe laser field (solid line) under the coupling laser modulation (dashed line) at different switching periods: $50/\gamma_{21}$ (**a**, **b**) and $5/\gamma_{21}$ (**c**, **d**). The other parameters are $\Omega_{p0}=0.2\gamma_{21}$, $\Omega_{c0}=10\gamma_{21}$ and $\Delta_p=\Delta_c=0$

$$\Omega_c^{(i)}(\tau)=\Omega_{c0}\left\{1-0.5\left[\tanh(\alpha_i\tau-4)-\tanh(\alpha_i\tau-14)+\tanh(\alpha_i\tau-24)-\tanh(\alpha_i\tau-34)\right]\right\} \tag{12}$$

with $\alpha_i=2.0$ or 0.4 $(i=1,\ 2)$ representing the switching period is $5/\gamma_{21}$ or $50/\gamma_{21}$, respectively.

In Fig. 4, we investigate the influence of the coupling intensity Ω_{c0} on the probe switching by fixing the laser parameters at $f(\xi=0,\tau)=1, \Omega_{p0}=0.2\gamma_{21}, \Delta_p=\Delta_c=0$ and period as $50/\gamma_{21}$, and plotting the time evolution of the probe laser field for different coupling

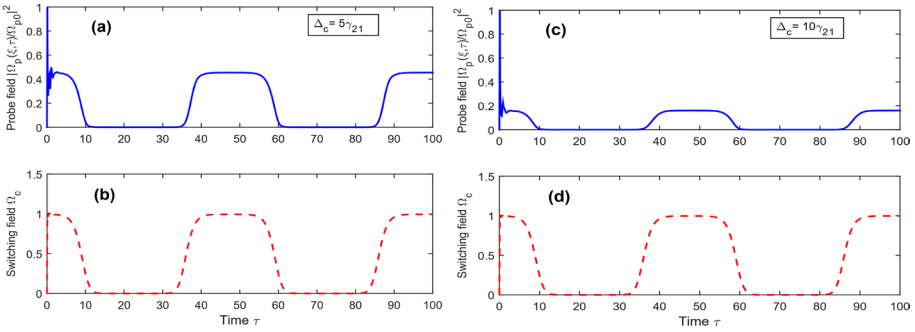

Fig. 6 Time evolution of the probe laser field (solid line) under the coupling laser modulation (dashed line) at different coupling frequency detuning: $\Delta_c = 5\gamma_{21}$ (**a**, **b**) and $\Delta_c = 10\gamma_{21}$ (**c**, **d**). The other parameters are given by $\Omega_{p0} = 0.2\gamma_{21}$, $\Omega_{c0} = 5\gamma_{21}$, $\Delta_p = 0$ and period as $50/\gamma_{21}$

laser field intensities: $\Omega_{c0} = 5\gamma_{21}$ (a–b), $\Omega_{c0} = 10\gamma_{21}$ (c–d), $\Omega_{c0} = 15\gamma_{21}$ (e–f), and $\Omega_{c0} = 20\gamma_{21}$ (g-h). It demonstrates that the probe field (continuous wave) is synchronously switched to a square pulse versus modulation of the coupling field. The switching efficiency may be defined as $\eta = (I_{on} - I_{off})I_{in}$, here I_{in} is the incident light intensity, I_{on} is the transmitted intensity when the switch is closed (turn on), and I_{off} is the transmitted intensity when the switch is open (turn off). For perfect switching, $\eta = 1$ ($I_{on} = I_{in}$ and $I_{off} = 0$). As shown in Fig. 4, we see that the coupling laser intensity has no effect on the switching period (switching time) but it significantly affects the switching efficiency. Indeed, the coupling laser intensity is small (Fig. 4a), the switching efficiency is also low (about 80%), which means about 20% of the probe field is absorbed by the medium. However, as the coupling field intensity increases, the switching efficiency of the probe field increases significantly and reaches 100% (Fig. 4g). At the same time, the oscillations on the front edge of the probe pulse are also significantly reduced, i.e., the probe pulse becomes more stable as the coupling intensity increases. These phenomena can be explained based on Fig. 2 that when the coupling intensity increases, the depth and width of the EIT window also increase.

In Fig. 5, we consider the influence of the switching period on the probe switching by fixing the laser parameters at $f(\xi = 0, \tau) = 1$, $\Omega_{p0} = 0.2\gamma_{21}$, $\Delta_p = \Delta_c = 0$ and $\Omega_{c0} = 10\gamma_{21}$, and plotting the time evolution of the probe laser field for different switching periods: switching period $= 50/\gamma_{21}$ (a–b) and switching period $= 5/\gamma_{21}$ (c–d). As shown in Fig. 5, with switching period is $50/\gamma_{21}$, the probe field (cw) is switched to a nearly square pulse shape. However, as the switching period decreases from $50/\gamma_{21}$ to $5/\gamma_{21}$, the front-edge oscillations increase significantly (Fig. 5c) and disturb the nearly square shape of the switching probe pulse. This physical phenomenon can be explained as follows: when the pulse period is small, the pulse width (in frequency units) is large, therefore the probe pulse may not be completely in the spectral region of the EIT window so that the probe pulse may be broken due to absorption or anomalous dispersion. When the pulse period is large enough, the pulse width is smaller, and therefore the probe pulse can be completely inside the transparent spectral region. Moreover, the medium needs a delay time for the EIT formation when the coupling field on and off switch. This delay time is the main factor that generates the probe-transmitted spectrum oscillation.

Finally, in Fig. 6, we investigate the influence of the coupling frequency detuning on the probe switching by fixing the laser parameters at $f(\xi = 0, \tau) = 1 \Omega_{p0} = 0.2\gamma_{21}$, $\Delta_p = 0$, $\Omega_{c0} = 10\gamma_{21}$ and period as $50/\gamma_{21}$, and plotting the time evolution of the probe laser field

for different coupling frequency detuning: $\Delta_c = 5\gamma_{21}$ (a–b) and $\Delta_c = 10\gamma_{21}$ (c–d). The figure shows that as the coupling frequency detuning increases, the EIT window is also gradually moved away from the resonance region, so the probe laser pulse is absorbed more strongly (at resonant frequency). This reduces the probe switching efficiency significantly as inllustrated in Fig. 6c.

4 Conclusion

All-optical switching was performed in a three-level V-type atomic medium under EIT condition. In this model, we have used the coupling laser field to create both the EIT and optical switching for the probe laser field. Accordingly, the continuous-wave probe laser field is modulated by the coupling laser field into a near-square pulse. The influences of the coupling intensity and frequency as well as the switching period on the switching behavior of the probe field were also studied. It is proved that as the coupling intensity increases, the depth and width of the EIT window increase, so the switching efficiency is also increased and the switching pulse becomes more stable. As the coupling frequency detuning increases, the EIT window is moved away from the resonance frequency, so the probe field is strongly absorbed and the switching efficiency is also reduced. The switching efficiency also decreases with the reduction of the switching period. The model may be helpful for experimental observation and applications in optical devices.

Author contributions HMD and LTYN conceived the presented idea; HMD, LVD, and LTYN developed the theory and performed the analytic calculations. All authors co-wrote the paper, discussed the results, and contributed to the final manuscript.

Funding This research was funded by Vingroup Innovation Foundation (VINIF) under project code VINIF.2022.DA00076 and Postdoctoral Scholarship Programme of Vingroup Innovation Foundation (VINIF) code VINIF.2022.STS.52.

Data availability The data that support the findings of this study are available from the corresponding author upon reasonable request.

Declarations

Conflict of interest The authors have no known competing financial interests or personal relationships that could have appeared to influence the work reported in this paper.

References

Anh, N.T., Thanh, T.D., Bang, N.H., Dong, H.M.: Microwave-assisted all-optical switching in a four-level atomic system. Pramana J. Phys. **95**, 37 (2021)

Antón, M.A., Carreño, F., Calderón, O.G., Melle, S., Gonzalo, I.: Optical switching by controlling the double-dark resonances in a N-tripod five-level atom. Opt. Commun. **281**, 6040–6048 (2008)

Arkhipkin, V.G., Timofeev, I.V.: Adiabatic propagation of short pulded under conditions of electromagnetically induced transparency. Quan. Electron. **30**, 180–184 (2000)

Bai, Z., Huang, G.: Enhanced third-order and fifth-order Kerr nonlinearities in a cold atomic system via Rydberg-Rydberg interaction. Opt. Exp. **24**, 4442–4461 (2016)

Bang, N.H., Doai, L.V., Khoa, D.X.: Controllable optical properties of multiple electromagnetically induced transparency in gaseous atomic media. Commun. Phys. **28**, 1–33 (2019)

Boller, K.J., Imamoglu, A., Harris, S.E.: Observation of electromagnetically induced transparency. Phys. Rev. Lett. **66**, 2593 (1991)
Brown, A.W., Xiao, M.: All-optical switching and router based on an electromagnetically induced absorption grating. Opt. Lett. **30**(7), 699–701 (2005)
Buica, B., Nakajima, T.: Propagation of two short laser pulse trains in a Λ-type three level medium under conditions of electromagnetically induced transparency. Opt. Commun. **332**, 59 (2014)
Doai, L.V., Phuong, L.T.M., Anh, N.T., Son, D.H., Khoa, D.X., Sau, V.N., Bang, N.H.: A comparative study of optical bistability in three-level EIT configurations. Commun. Phys. **28**(2), 127–138 (2018)
Dong, H.M., Bang, N.H.: Controllable optical switching in a closed-loop three-level lambda system. Phy. Scr. **94**, 115510 (2019)
Dong, H.M., Doai, L.V., Bang, N.H.: Pulse propagation in an atomic medium under spontaneously generated coherence, incoherent pumping, and relative laser phase. Opt. Commun. **426**, 553–557 (2018)
Dong, H.M., Doai, L.V., Sau, V.N., Khoa, D.X., N.H., Bang: Propagation of laser pulse in a three-level cascade atomic medium under conditions of electromagnetically induced transparency. Photon. Lett. Pol. **3**, 73 (2016a)
Dong, H.M., Doai, L.V., Sau, V.N., Khoa, D.X., Bang, N.H.: Propagation of laser pulse in a three-level cascade atomic medium under conditions of electromagnetically induced transparency. Photon. Lett. Pol. **8**, 73 (2016b)
Dong, H.M., Nga, L.T.Y., Bang, N.H.: Optical switching and bistability in a degenerated two-level atomic medium under an external magnetic field. Appl. Opt. **58**, 4192 (2019)
Eberly, J.H.: Transmission of dressed fields in three-level media. Quantum Semiclass. Opt. **7**, 373–384 (1995)
Eisaman, M.D., André, A., Masou, F., Fleischhauer, M., Zibrov, A.S., Lukin, M.D.: Electromagnetically induced transparency with tunable single-photon pulses. Nature **438**, 837–841 (2005)
Fountoulakis, A., Terzis, A.F., Paspalakis, E.: All-optical modulation based on electromagnetically induced transparency. Phys. Lett. A **374**, 3354–3364 (2010)
Harris, S.E.: Electromagnetically induced transparency. Phys. Today **50**(7), 36–42 (1997)
Harris, S.E., Luo, Z.-F.: Preparation energy for electromagnetically induced transparency. Phys. Rev. A **52**, R928 (1995)
Huang, G., Jiang, K., Payne, M.G., Deng, L.: Formation and propagation of coupled ultraslow optical soliton pairs in a cold three-state double–system. Phys. Rev. E **73**, 056606 (2006)
Ishikawa, H.: Ultrafast All-Optical Signal Processing Devices. Wiley, Singapore (2008)
Kasapi, A., Jain, M., Gin, G.Y., Harris, S.E.: Electromagnetically induced transparency: propagation dynamics. Phys. Rev. Lett **74**, 2447–2450 (1995)
Khoa, D.X., Doai, L.V., Son, D.H., Bang, N.H.: Enhancement of self-Kerr nonlinearity via electromagnetically induced transparency in a five-level cascade system: an analytical approach. J. Opt. Soc. Am. B **31**(6), 1330 (2014)
Khoa, D.X., Dong, H.M., Doai, L.V., Bang, N.H.: Propagation of laser pulse in a three-level cascade inhomogeneously broadened medium under electromagnetically induced transparency conditions. Optik **131**, 497 (2017b)
Khoa, D.X., Trung, L.C., Thuan, P.V., Doai, L.V., Bang, N.H.: Measurement of dispersive profile of a multiwindow electromagnetically induced transparency spectrum in a Doppler-broadened atomic medium. J. Opt. Soc. Am. B Josab. **34**(N6), 1255–1263 (2017a)
Kiffner, M., Dey, T.N.: Dynamical control of pulse propagation in electromagnetically induced transparency. Phys. Rev. A **79**, 023829 (2009)
Li, J.H., Yu, R., Wu, Y.: Propagation of magnetically controllable lasers and magneto-optic dual switching using nitrogen-vacancy centers in diamond. J. Appl. Phys. **113**, 103104 (2013)
Qi, Y., Niu, Y., Zhou, F., Peng, Y., Gong, S.: Phase control of coherent pulse propagation and switching based on electromagnetically induced transparency in a four-level atomic system. J. Phys. B at. Mol. Opt. Phys. **44**, 085502 (2011)
Qi, Y., Zhou, F., Yang, J., Niu, Y., Gong, S.: Controllable twin laser pulse propagation and dual-optical switching in a four-level quantum dot nanostructure. J. Opt. Soc. Am. B **30**, 1928 (2013)
Schmidt, H., Ram, R.J.: All-optical wavelength converter and switch based on electromagnetically induced transparency. Appl. Phys. Lett. **76**, 3173 (2000)
Si, L.G., Lu, X.Y., Hao, X., Li, J.H.: Dynamical control of soliton formation and propagation in a Y-type atomic system with dual ladder-type electromagnetically induced transparency. J. Phys. B at. Mol. Opt. Phys. **43**, 065403 (2010)
Wan, R.G., Kou, J., Kuang, S.Q., Jiang, L., Gao, J.Y.: Controlled light-pulse propagation via dynamically induced double photonic band gap. Opt. Exp. **18**, 15591–15596 (2010)

Wang, H., Goorskey, D., Xiao, M.: Enhanced Kerr nonlinearity via atomic coherence in a three-level atomic system. Phys. Rev. Lett. **87**, 073601 (2001)
Wei, X., Zhang, J., Zhu, Y.: All-optical switching in a coupled cavity-atom system. Phys. Rev. A **82**, 033808 (2010)
Wu, Y., Yang, X.: Electromagnetically induced transparency in V-, Λ-, and cascade-type schemes beyond steady-state analysis. Phys. Rev. A **71**(5), 053806 (2005)
Yavuz, D.D.: All-optical femtosecond switch using two-photon absorption. Phys. Rev. A **74**, 053804 (2006)
Ying, K., Niu, Y., Chen, D., Cai, H., Qu, R., Gong, S.: Observation of multi-electromagnetically induced transparency in V-type rubidium atoms. J. Mod. Opt. **61**, 631–635 (2014)
Yu, R., Li, J., Huang, P., Zheng, A., Yang, X.: Dynamic control of light propagation and optical switching through an RF-driven cascade-type atomic medium. Phys. Lett. A **373**, 2992 (2009)